# Electronic Supplementary Information

## Facile synthesis of effective Ru nanoparticles on carbon by adsorption-low temperature pyrolysis strategy for hydrogen evolution

Caili Xu, Mei Ming, Qi Wang, Chun Yang, Guangyin Fan*, Yi Wang, Daojiang Gao, Jian Bi, and Yun Zhang*

College of Chemistry and Materials Science, Sichuan Normal University, Chengdu 610068, China

E-mail: fanguangyin@sicnu.edu.cn (G.Y. Fan) and zhangyun@sicnu.edu.cn (Y. Zhang).

This file includes Chemicals and Materials, Characterization, Figs. S1-S7, and Tables. S1-S3.

## Chemicals and Materials

Dodecacarbonyltriruthenium ($Ru_3(CO)_{12}$, 99%), AB with 90% purity, and nafion (5 wt%) were supplied by Sigma-Aldrich. Acetone and ethyl alcohol were brought from Aladdin Industrial Inc. Pt/C (Vulcan carbon) with a metal loading of 20 wt% was provided by Alfa Aesar. Carbon black (Vulcan®XC-72) was acquired from Cabot Corp. No further treatment was performed on the received chemicals and materials. Ultrapure water (resistivity: 18.2 MΩ cm) was directly applied during sample preparations and catalytic activity tests.

## Characterization

Transmission electron microscopy (TEM) and high-resolution TEM studies were conducted using a JEOL JEM-2100F instrument. The crystal structure of the samples was measured through X-ray diffraction (XRD) using a PANalytical X'Pert diffractometer using Cu K□ radiation source (λ=1.54178 Å, 40 kV and 40 mA). X-ray photoelectron spectroscopy (XPS) experiments were performed using a Thermo ESCALAB 250 Axis Ultra analyzer with an Al Kα radiation source (hν= 1486.6 eV). The specific surface area (SSA) and pore size distribution of the samples were characterized using an automated gas sorption analyzer (Quantachrome, Autosorb-IQ).

**Figure S1.**

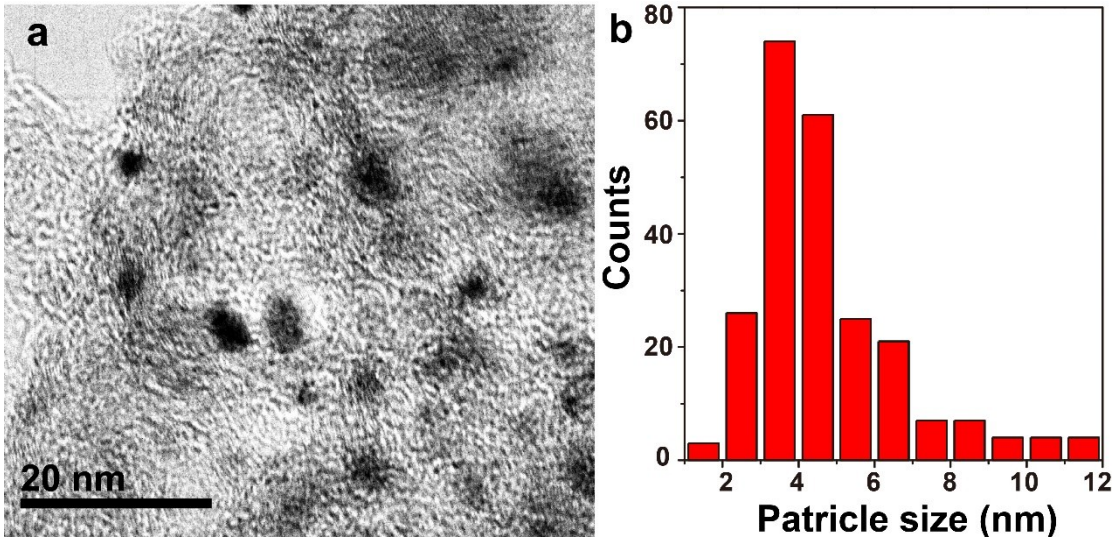


Fig. S1 (a) TEM image of Ru/C-700, (b) particle size distribution of Ru/C-700.

**Figure S2.**

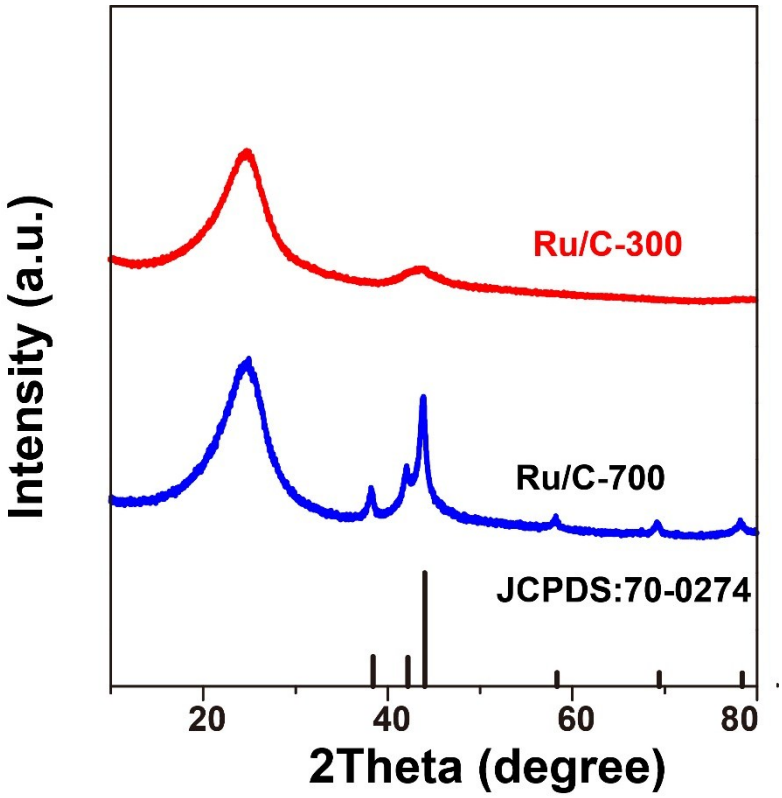


Fig. S2 XRD patterns of Ru/C-300 and Ru/C-700.

**Figure S3.**

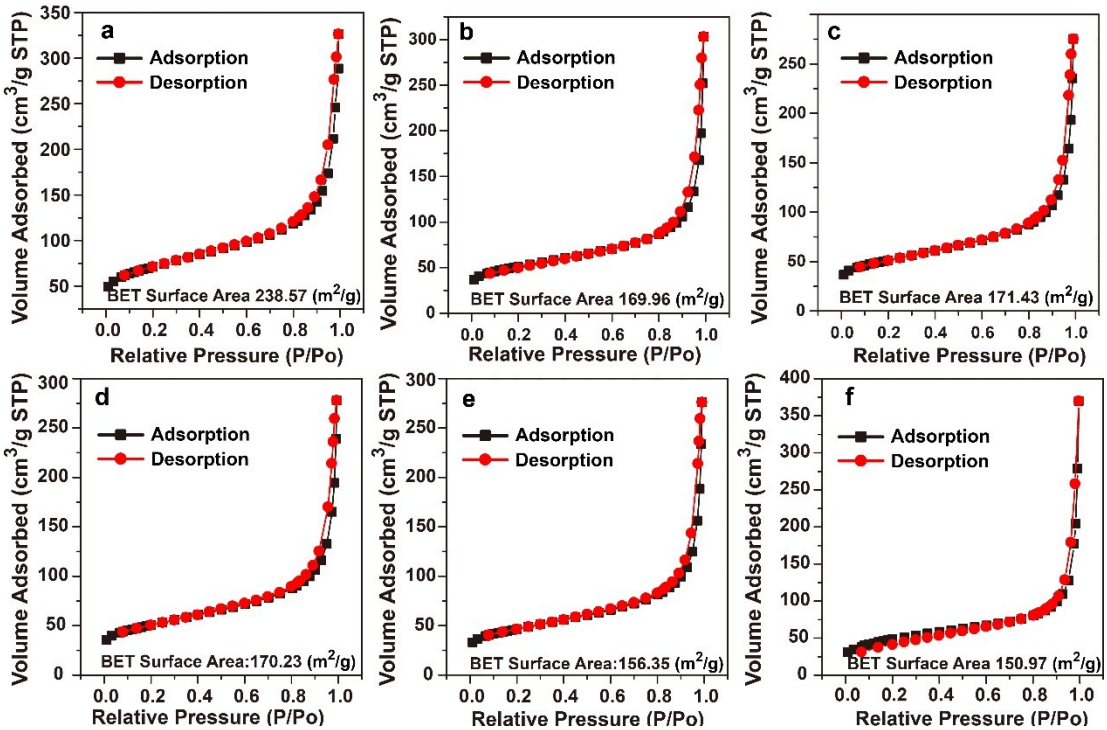


Fig. S3 BET surface areas of (a) carbon, (b) Ru/C-200, (c) Ru/C-300, (d) Ru/C-400, (e) Ru/C-500 and (f) Ru/C-700.

**Figure S4.**

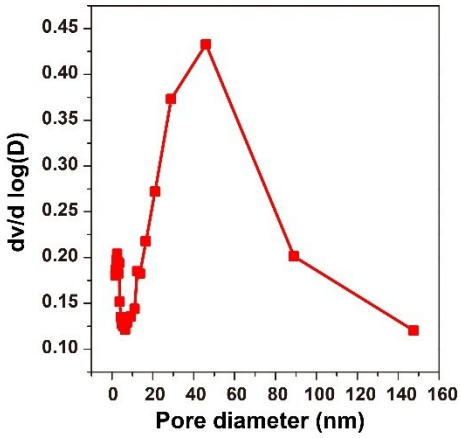


Fig. S4 Pore size distribution of the carbon support.

**Figure S5.**

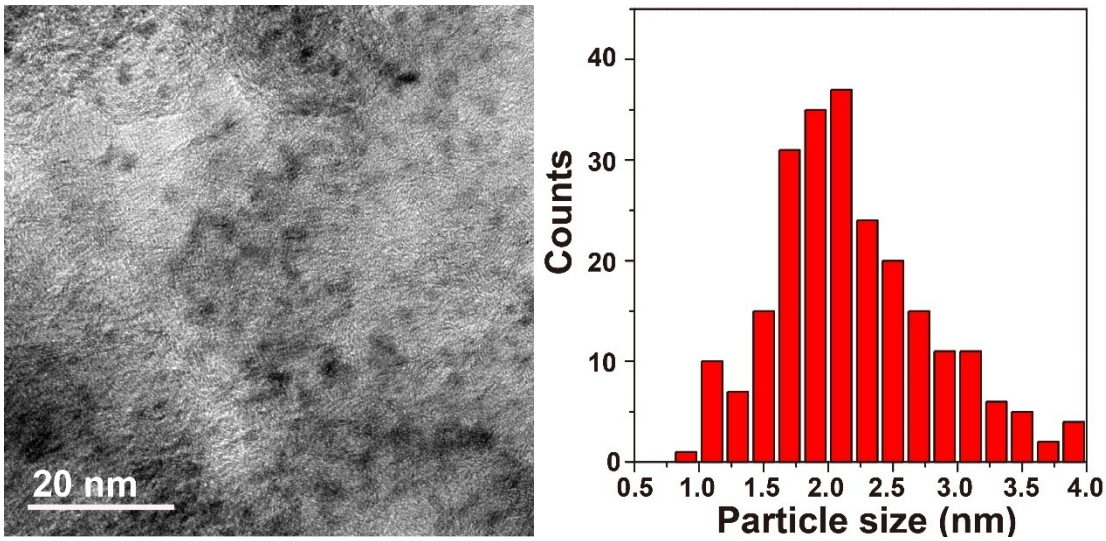


Fig. S5 (a) TEM image and (b) particle size distribution of Ru/C-300 after 1000 cycles.

**Figure S6.**

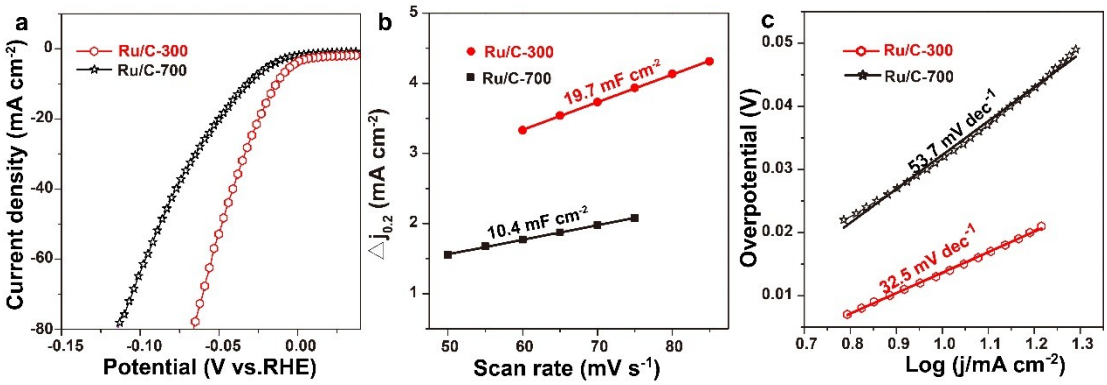


Fig. S6 (a) LSV curves of Ru/C-300 and Ru/C-700, (b) the capacitive current determined by plotting as a function of scan rates, (c) Tafel slopes of Ru/C-300 and Ru/C-700.

**Figure S7.**

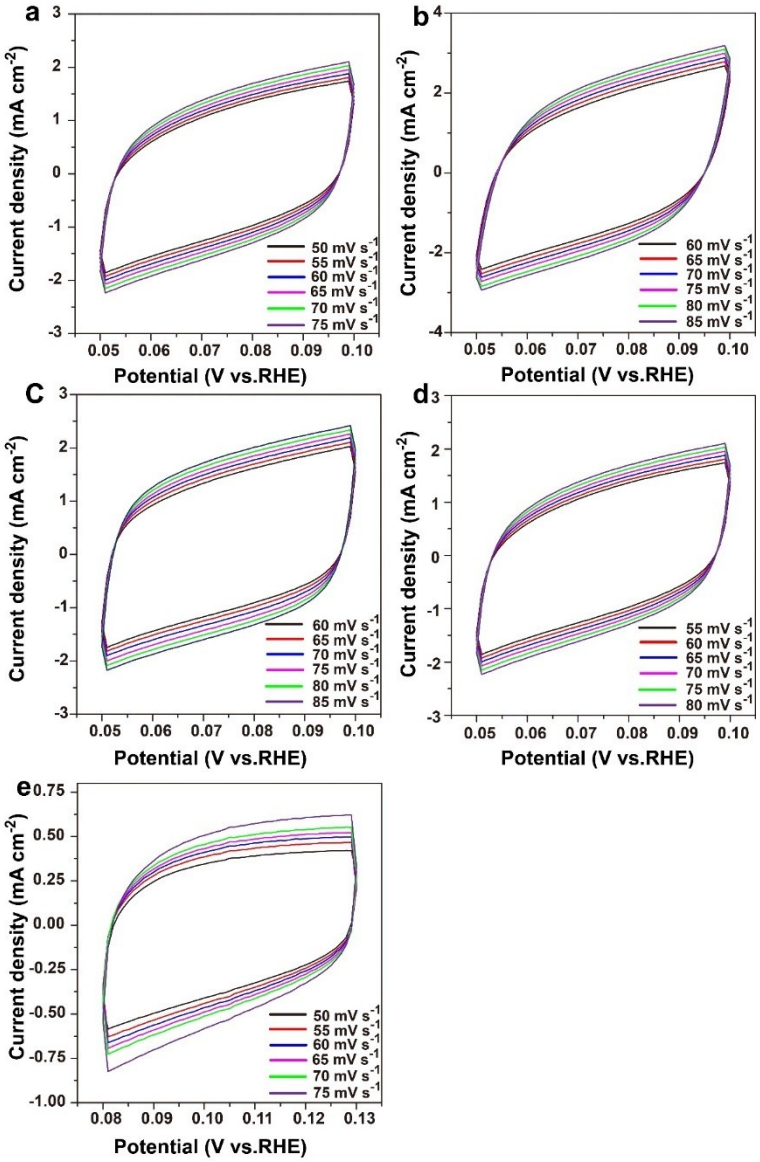


Fig. S7 CV curves measured at different scan rates in 1.0 M KOH for as-prepared catalysts (a) Ru/C-200, (b) Ru/C-300, (c) Ru/C-400, (d) Ru/C-500, (e) Ru/C-700.

**Table S1. Textural properties of the catalysts.**

| Catalysts | BET surface area ($m^2/g$) | Pore volume ($cm^3/g$) |
|---|---|---|
| Ru/C-200 | 169.96 | 0.49 |
| Ru/C-300 | 171.43 | 0.41 |
| Ru/C-400 | 170.23 | 0.42 |
| Ru/C-500 | 156.35 | 0.42 |
| Ru/C-700 | 150.96 | 0.46 |

**Table S2. Comparison of HER activities with reported literature**

| Electrocatalysts | Overpotential at 10 mA·cm$^{-2}$(mV) | Electrolyte solution | Tafel Polts (mV dec$^{-1}$) | Ref. |
|---|---|---|---|---|
| Ru/NG-750 | 8 | 1.0 M KOH | 30 | 1 |
| | 53 | 0.5 M $H_2SO_4$ | 44 | |
| $RuP_2$@NPC | 52 | 1.0 M KOH | 69 | 2 |
| | 38 | 0.5 M $H_2SO_4$ | 38 | |
| | 57 | 1.0 M PBS | 87 | |
| RuCo@NC | 28 | 1.0 M KOH | 31 | 3 |
| Ru/$C_3N_4$/C | 79 | 1.0 M KOH | — | 4 |
| Ru@$C_2N$ | 17 | 1.0 M KOH | 38 | 5 |
| | 13.5 | 0.5 M $H_2SO_4$ | 30 | |
| Ru-$MoO_2$ | 29 | 1.0 M KOH | 31 | 6 |
| | 55 | 0.5 M $H_2SO_4$ | 44 | |
| Ru/GLC | 35 | 0.5 M $H_2SO_4$ | 46 | 7 |
| Ru@CN | 32 | 1.0 M KOH | 53 | 8 |
| Ru/$MoS_2$/CP | 13 | 1.0 M KOH | 60 | 9 |
| | 96 | 0.5 M $H_2SO_4$ | — | |
| NiCoP@Ru | 52 | 1.0 M KOH | 50 | 10 |
| | 49 | 0.5 M $H_2SO_4$ | 48 | |
| Ru nanosheets | 20 | 0.5 M $H_2SO_4$ | 46 | 11 |
| Ru/C-300 | 14 | 1.0 M KOH | 32.5 | This work |

**Table S3. Comparison of catalytic activity of previously reported ruthenium-based catalysts applied for AB hydrolysis**

| Catalysts | TOF ($mol \cdot H_2$ $(min \cdot mol_{Ru})^{-1}$) | Ea (kJ/mol) | References |
|---|---|---|---|
| Ru/carbon | 670 | 14.3 | [12] |
| $Ru/Al_2O_3$-NFs | 327 | 36.1 | [13] |
| $Ru(0)/TiO_2$ | 241 | 70 | [14] |
| $Ru@SiO_2$ | 200 | 38.2 | [15] |
| $Ru@Al_2O_3$ | 83.3 | 48 | [16] |
| $Ru^0/CeO_2$ | 361 | 51 | [17] |
| $Ru^0/ZrO_2$ | 173 | 58 | [18] |
| $Ru/g\text{-}C_3N_4$ | 313 | 37.4 | [19] |
| Ru/ND | 229 | 50.7 | [20] |
| Ru/Graphene | 600 | 12.7 | [21] |
| Ru@X-NW | 135 | 77 | [22] |
| RuCu/graphene | 135 | 30.59 | [23] |
| $Ru^0/HfO_2$ | 170 | 65 | [24] |
| Ru/C | 429.5 | 34.8 | [25] |
| PtRu@PVP | 308 | 56.3 | [26] |
| Ru(0)@MWCNT | 329 | 33 | [27] |
| $Ru/TiO_2(B)$ | 303 | 45.6 | [28] |
| Ru@Ni/graphene | 339.5 | 36.59 | [29] |
| RuRh@PVP | 386 | 47.4 | [30] |
| Ru/C-300 | 643 | 38.7 | This work |

## References:


1. R. Ye, Y. Liu, Z. Peng, T. Wang, A. S. Jalilov, B. I. Yakobson, S. H. Wei and J. M. Tour, *ACS Appl. Mater. Interfaces*, 2017, **9**, 3785-3791.
2. Z. Pu, I. S. Amiinu, Z. Kou, W. Li and S. Mu, *Angew Chem. Int. Ed.*, 2017, **56**, 11559-11564.
3. J. Su, Y. Yang, G. Xia, J. Chen, P. Jiang and Q. Chen, *Nat. Commun.*, 2017, **8**, 14969.
4. Y. Zheng, Y. Jiao, Y. Zhu, L. H. Li, Y. Han, Y. Chen, M. Jaroniec and S. Z. Qiao, *J. Am. Chem. Soc.*, 2016, **138**, 16174-16181.
5. J. Mahmood, F. Li, S. M. Jung, M. S. Okyay, I. Ahmad, S. J. Kim, N. Park, H. Y. Jeong and J. B. Baek, *Nat. Nanotechnol.*, 2017, **12**, 441-446.
6. P. Jiang, Y. Yang, R. Shi, G. Xia, J. Chen, J. Su and Q. Chen, *J. Mater. Chem. A,* 2017, **5**, 5475-5485.
7. Z. Chen, J. Lu, Y. Ai, Y. Ji, T. Adschiri and L. Wan, *ACS Appl. Mater. Interfaces*, 2016, **8**, 35132-35137.
8. J. Wang, Z. Wei, S. Mao, H. Li and Y. Wang, *Energy Environ. Sci.*, 2018.
9. J. Liu, Y. Zheng, D. Zhu, A. Vasileff, T. Ling and S. Z. Qiao, *Nanoscale*, 2017, **9**, 16616-16621.
10. S. Liu, Q. Liu, Y. Lv, B. Chen, Q. Zhou, L. Wang, Q. Zheng, C. Che and C. Chen, *Chem. Commun.*, 2017, **53**, 13153-13156.
11. X. Kong, K. Xu, C. Zhang, J. Dai, S. Norooz Oliaee, L. Li, X. Zeng, C. Wu and Z. Peng, *ACS Catal.*, 2016, **6**, 1487-1492.
12. M. Navlani-García, K. Mori, A. Nozaki, Y. Kuwahara and H. Yamashita, *Appl. Catal., A,* 2016, **527**, 45-52.
13. M. Hu, H. Wang, Y. Wang, Y. Zhang, J. Wu, B. Xu, D. Gao, J. Bi and G. Fan, *Int. J. Hydrogen Energy,* 2017, **42**, 24142-24149.
14. S. Akbayrak, S. Tanyıldızı, İ. Morkan and S. Özkar, *Int. J. Hydrogen Energy,* 2014, **39**, 9628-9637.
15. Q. Yao, W. Shi, G. Feng, Z.-H. Lu, X. Zhang, D. Tao, D. Kong and X. Chen, *J. Power Sources*, 2014, **257**, 293-299.
16. H. Can and Ö. Metin, *Appl. Catal. B.*, 2012, **125**, 304-310.
17. S. Akbayrak, Y. Tonbul and S. Ozkar, *Dalton. Trans.*, 2016, **45**, 10969-10978.
18. Y. Tonbul, S. Akbayrak and S. Ozkar, *J. Colloid Interface Sci*, 2017, **513**, 287-294.
19. Y. Fan, X. Li, X. He, C. Zeng, G. Fan, Q. Liu and D. Tang, *Int. J. Hydrogen Energy,* 2014, **39**, 19982-19989.
20. G. Fan, Q. Liu, D. Tang, X. Li, J. Bi and D. Gao, *Int. J. Hydrogen Energy,* 2016, **41**, 1542-1549.
21. C. Du, Q. Ao, N. Cao, L. Yang, W. Luo and G. Cheng, *Int. J. Hydrogen Energy,* 2015, **40**, 6180-6187.
22. S. Akbayrak and S. Ozkar, *Dalton. Trans.*, 2014, **43**, 1797-1805.
23. N. Cao, K. Hu, W. Luo and G. Cheng, *J. Alloys Compd.*, 2014, **590**, 241-246.
24. E. B. Kalkan, S. Akbayrak and S. Özkar, *Mol. Catal.*, 2017, **430**, 29-35.
25. H. Liang, G. Chen, S. Desinan, R. Rosei, F. Rosei and D. Ma, *Int. J. Hydrogen Energy,* 2012, **37**, 17921-17927.
26. M. Rakap, *Appl. Catal., A,* 2014, **478**, 15-20.
27. S. Akbayrak and S. Ozkar, *ACS Appl. Mater. Interfaces*, 2012, **4**, 6302-6310.
28. Y. Ma, X. Li, Y. Zhang, L. Chen, J. Wu, D. Gao, J. Bi and G. Fan, *J. Alloys Compd.*, 2017, **708**, 270-277.

29. N. Cao, J. Su, W. Luo and G. Cheng, *Int. J. Hydrogen Energy,* 2014, **39**, 426-435.
30. M. Rakap, *J. Alloys Compd.*, 2015, **649**, 1025-1030.